QUANTIFICATION OF RADIATING SPECIES IN THE DIII-D DIVERTOR IN THE TRANSITION TO DETACHMENT USING EXTREME ULTRAVIOLET SPECTROSCOPY

A.G. McLEAN
Lawrence Livermore National Laboratory
Livermore, USA
Email: mclean@fusion.gat.com

S.L. ALLEN
M.E. FENSTERMACHER
A.E. JAERVINEN
C.J. LASNIER
G.D. PORTER
T. ROGNLIEN
C.M. SAMUELL
V.A. SOUKHANOVSKII
Lawrence Livermore National Laboratory
Livermore, USA

J. BOEDO
E.M. HOLLMANN
University of California, San Diego
San Diego, USA

A.W. LEONARD
A.L. MOSER
D. THOMAS
General Atomics
San Diego, USA

A. BRIESEMEISTER
Oak Ridge National Laboratory
Oak Ridge, USA

H.Q. WANG
Oak Ridge Associated Universities
Oak Ridge, USA

J.D. WATKINS
Sandia National Laboratory
Albuquerque, USA

M. GROTH
Aalto University
Espoo, Finland

Abstract

Experimental observations of extreme ultraviolet (EUV) resonance emissions in the divertor of DIII-D are used to quantitatively account for radiated power from molecular, atomic and ionized plasma constituents through the transition to detachment. Deuterium emission is found to be the primary emitter near the target scrape-off layer regions while the main impurity in DIII-D, carbon, is found to dominate the X-point region up the divertor legs. In an attached divertor, C emissions peak upstream of the strike point, while with a detached target, their emission region elongates radially. Species-resolved measurements are necessary to understand a shortfall in radiated power as modelled with 2D fluid codes on multiple tokamaks. The spectrometer fielded for this purpose is a SPRED (Survey, Poor Resolution, Extended Domain) observing the 500-1700Å region. A broad grating provides views of C II, III, and IV resonance emission lines as well as the D Lyman-α line, together accounting for >50% of the power radiated in the divertor. The divertor SPRED (DivSPRED) is mounted with a vertical line of sight into the machine coincident with boundary diagnostics including divertor Thomson scattering. Radiation not accounted

for by line emission is found primarily in the spectral region of the Lyman-Werner band system suggesting that radiated power from molecules may be significant and prominent in all divertor conditions.

1. INTRODUCTION

The Tokamak divertor provides conditions which are conducive to radiation of low-Z elements ($Z \leq 10$) via resonance emission lines – that is, those electron transitions whose lower state is the ground state. These resonance lines preferentially emit in the extreme ultraviolet (EUV) portion (10-120 nm) and the broader vacuum ultraviolet (VUV) portion of the EM spectrum (10-200 nm). Study of the EUV/VUV region offers a direct window into the primary radiating processes and constituents in a fusion plasma. In addition, emissions in this region offer a comprehensive set of validation data for boundary modeling codes simulating the divertor environment for interpretation of plasma performance and plasma-wall interactions. The ability to accurately predict the rates at which electronic excitation and de-excitation processes occur for resonance emissions in the EUV/VUV region, and their relatively overwhelming intensity compared to higher state transitions at visible or infrared wavelengths. In particular, recent modeling efforts for multiple Tokamaks including JET, ASDEX-U and DIII-D have been undertaken with multiple fluid-based simulation codes, each demonstrating a similar result: A shortfall in predicted radiation in the divertor region compared to that measured with bolometric-based diagnostics in each machine [1,2]. In response, an effort to install, operate, and calibrate an EUV/VUV spectrometer on DIII-D has been undertaken, allowing study of radiating species (atomic, ionic, and molecular) and absolute radiating intensity in the divertor through the transition to detachment. Results from analysis of these experiments are presented and discussed.

2. EXPERIMENTAL APPROACH

2.1. Divertor SPRED

Divertor SPRED (DivSPRED) is a McPherson Model 251 grazing incidence flat field grating spectrometer designed for Survey, Poor Resolution and Extended Domain (SPRED) observation of the EUV (10-120 nm) and VUV (10-200 nm) region [3,4]. This model spectrometer is commonly used for core SPRED observation in a radial midplane view of the 10-120 nm region, primarily to identify metallic impurities in tokamak devices, but was also fielded on DIII-D in the late 1990's for divertor observation [5-10]. It is in the EUV/VUV where resonant emission – those transitions whose lower level is the ground state of an atom or ion – of low charge states for low-Z elements are prominently found, especially in the region of 50-160 nm for the typical light constituents of a DIII-D plasma. These elements include deuterium and carbon, as well as helium, lithium and boron (used for wall conditioning), and injected impurities such as nitrogen, neon, and argon used for detachment onset and control. Together, a small number of resonant lines including the D I Lyman-α, 121.5 nm, C III, 97.7 nm, and C IV, 155.0 nm add up to a significant portion of the total power radiated by the plasma in the DIII-D divertor. By studying these emissions directly, potential complexities of higher-n transitions can be avoided. As well, measured absolute intensity of integrated emissions observed by DivSPRED can be compared directly to bolometric diagnostics. Finally, the brightness of these emissions allows study of radiating species with high time resolution through transients like edge-localized modes (ELMs).

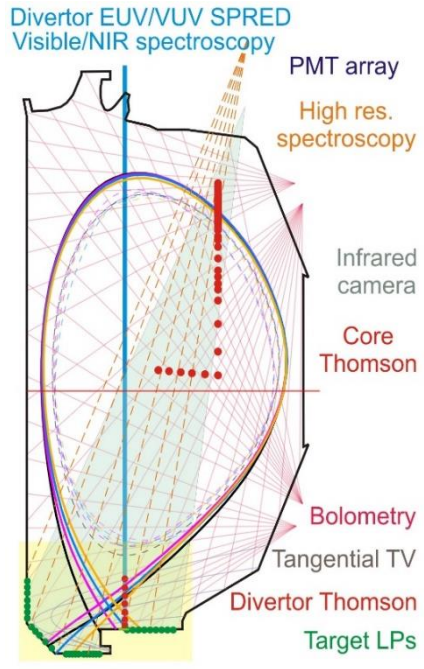

FIG. 1. Diagnostic suite for the DIII-D divertor used for radiation studies.

DivSPRED includes a CuI photocathode to convert VUV photons to electrons, a 40 mm diameter high voltage single-plate Chevron Multichannel Plate (MCP) with 12 um pores for electron multiplication, followed by a P43 phosphor anode to convert electrons back to photons, but at a singular visible wavelength (550 nm, in the green). The spectrometer itself is directly open to the DIII-D vacuum but separately pumped to maintain high vacuum conditions within the chamber during gas injection in the vessel for plasma density control. The output from the phosphor is transmitted through a fused silica fiber-optic taper which both acts as the vacuum interface and reduces the image diameter to 25 mm for monitoring by a scientific camera. Wherein the past a camera would be mated directly to the taper itself, in the current application a highly sensitive camera – an electron-multiplying scientific CCD – is linked to the taper via an optical relay composed of a conjugate lens pair to collimate and then focus the light,

and a mirror between them in order to allow the camera to be fully shielded from direct line-of-sight gamma rays from the DIII-D device using a 2" thick lead shield box. Additionally, the full spectrometer and detector is shielded from neutrons using a 4-6" thickness of 5% boronated polyethylene, and from magnetic fields using 0.5" thick low-carbon steel around each of the camera and MCP assembly.

Due to the poor and difficult-to-predict performance of mirrors in the EUV region, DivSPRED was installed on DIII-D at the 285° toroidal, V+1/R=1.485 m port, with a direct line-of-sight into the lower divertor where most divertor characterization studies are performed due to the presence of a multitude of other supporting diagnostic systems observing that region of the plasma (FIG. 1). Additionally, the view was designed to terminate on a graphite tile on the plasma-facing surface to ensure that effects of local erosion and recycling were properly represented within the view chord. Due to the distance between the grating inside the instrument above DIII-D and the lower divertor (5.39 meters), the radial width of the view chord on the floor due to the grating (ruled dimensions of 10 × 22 mm) and entrance slit (25 μm × 1 mm) alone would be 23 cm. To reduce this range for purposes of radial identification of emission features as the target plasma is swept across the DivSPRED view, a pre-slit is used with a radial width of 0.25 mm, leading to a view chord width of 3.8 cm and an effective f/# of ~100. While significantly constrained, this width introduces some 'smear' or convolution of the emission profile with this observationally-averaged width. To account for this effect, however, a similar viewing geometry is adopted for use in a synthetic diagnostic that extracts emission data from results of modeling codes such as UEDGE, SOLPS, and EDGE-2D.

2.2. **Supporting diagnostics**

Several associated diagnostics complement the capabilities of DivSPRED on DIII-D. This includes the Divertor Thomson scattering (DTS) system, unique in tokamaks worldwide as of 2018, that provides an 8-channel vertical array of co-located electron temperature and density measurements in the lower divertor. Used in conjunction with sweeping of the X-point and strike points, the DTS system may be applied to characterize the plasma in 2D space and provides parameterization critical for interpretation of DivSPRED results like emission species and extent along the 1D viewing chord.

TABLE 1. SPECTROSCOPY DIAGNOSTIC ARRAY

Diagnostic	**DivSPRED**	**VisFX Blue**	**VisFX Red**	**MDS**	**NIRS**
Spectrometer	McPherson Model 251 FL=0.33 m	Ocean Optics Ocean FX FL=0.1 m	Ocean Optics Ocean FX FL=0.1 m	McPherson Model 201 FL=1.3 m	Princeton Instrum. Acton SP2500 FL=0.5 m
Grating	290 gr/mm 450 gr/mm 2105 gr/mm	2400 gr/mm	1800 gr/mm	1200 gr/mm	300 gr/mm 600 gr/mm 1200 gr/mm
***f*/#**	14 reduced to ~100 with preslit	4.0	4.0	9.4	6.5
Slit width	25 μm	25 μm	25 μm	20 μm	50 μm
Range	47-170 nm 10-110 nm 10-30 nm	395-518 nm	520-695 nm	380-650 nm (scanable)	600-2500 nm 620-2500 nm 800-1600 nm
Bandwidth (median)	127 nm 100 nm 20 nm	123 nm	175 nm	8 nm/setting	155 nm 68 nm 24 nm
Detector (all 16-bit A/D)	Princeton Instruments ProEM+ 1600x200 (EMCCD)	Hamamatsu S11639-01 (CMOS)	Hamamatsu S11639-01 (CMOS)	Princeton Instruments PI-MAX4 (ICCD)	Princeton Instruments OMA V (InGaAs PDA, LN_2 cooled)
Spectral pixels	1600	2136	2136	1024	1024
Dispersion (nm/pixel)	0.077 nm/pixel	0.059 nm/pixel	0.080 nm/pixel	0.0078 nm/pixel	0.15 nm/pixel 0.066 nm/pixel 0.023 nm/pixel
Optical resolution	0.95 nm (12 pixels)	0.27 nm (4.5 pixels)	0.36 nm (4.5 pixels)	0.03 nm (3.8 pixels)	0.43 nm (2.9 pixels) 0.31 nm (4.7 pixels) 0.07 nm (3.0 pixels)
Integration time/frame rate	1.836 ms 542 Hz	0.1-98 ms 1-300 Hz	0.1-98 ms 1-300 Hz	1-10 ms 10-100 Hz	0.1-998 ms 1-900 Hz
Machine location	285 V+1	150 V+1	150 V+1	150 R+2	150 V+1

Visible spectroscopy is also available in both high resolution format via the Multichord Divertor Spectrometer (MDS) diagnostic, as well as broadband visible spectrometers co-located with the DivSPRED view along the same V+1 vertical view. The latter diagnostic was installed primarily to provide a means to cross-calibrate the DivSPRED *in-situ* using the branching ratio technique employed for similar VUV instruments previously for emission lines with the same upper level [11-18], and employs a pair of Ocean Optics FX symmetrical crossed *f*/4 Czerny-Turner spectrometers spanning 395-518 and 520-690 nm. Near infrared (NIR) spectroscopy is also available and co-located on the same view to access emission lines in the 600-2500 nm region, particularly high-n emissions of D (the Paschen series) and neutral/low charge-state impurity emissions.

Each of the four visible/NIR range spectrometers were independently calibrated for absolute sensitivity using an Optronics Labsphere from inside the DIII-D vessel after the end of the FY2018 experimental operations campaign. While DivSPRED employs a direct view into the DIII-D vacuum, each of the other spectrometers are coupled to a vessel port UHV window by large diameter (600-1000 um diameter) fused silica fiber optics and a lens. The lens focal length – typically 75-100 mm – is chosen to give the device a spot size on the lower divertor floor/shelf equal to that of DivSPRED. Together, these instruments provide calibrated spectral radiance data for all species within DIII-D across the majority of the EM spectrum from EUV to NIR wavelengths, and with several 100 Hz time resolution.

2.3. Experiments

Discharges were run on DIII-D in a broad variety of conditions in both L-mode and H-mode with injected power from 0.5-13 MW with the DivSPRED and supporting spectroscopy suite in operation. In particular, long, steady discharges with single parameter variation were run at various values of B_T, I_P, P_{inj}, and B_T field direction (i.e., ion B×▽B into/out of the divertor). Two key types of plasma discharges were run in particular; those with a slow ramp of the line-averaged density ($<n_e>$) with steady strike point locations on the lower divertor shelf/floor, and those at a constant $<n_e>$ but with sweeping of the strike points. The former discharges are used to characterize conditions at different points of the target or X-point at increasing degrees of detachment, while the latter is used to study the full divertor in the radial direction with spectrometers that are inherently 1D diagnostics. Characteristic data from each type of discharge are shown in FIG. 2. In particular, the swept discharge shown in black demonstrates that a sweep of the divertor targets allows inspection of both the outer and inner target by the DivSPRED and other supporting diagnostics (at R=1.485 m). As well, the density ramp discharge (shown in red) demonstrates that the divertor plasma spans conditions of a well attached target ($T_{e,OSP}$~20 eV and $n_{e,OSP}$~5x10^{19}/m^3) to well detached ($T_{e,OSP}$~0.4 eV and $n_{e,OSP}$>5x10^{20}/m^3) at the highest core plasma densities achieved (n/n_{GW}~1.0).

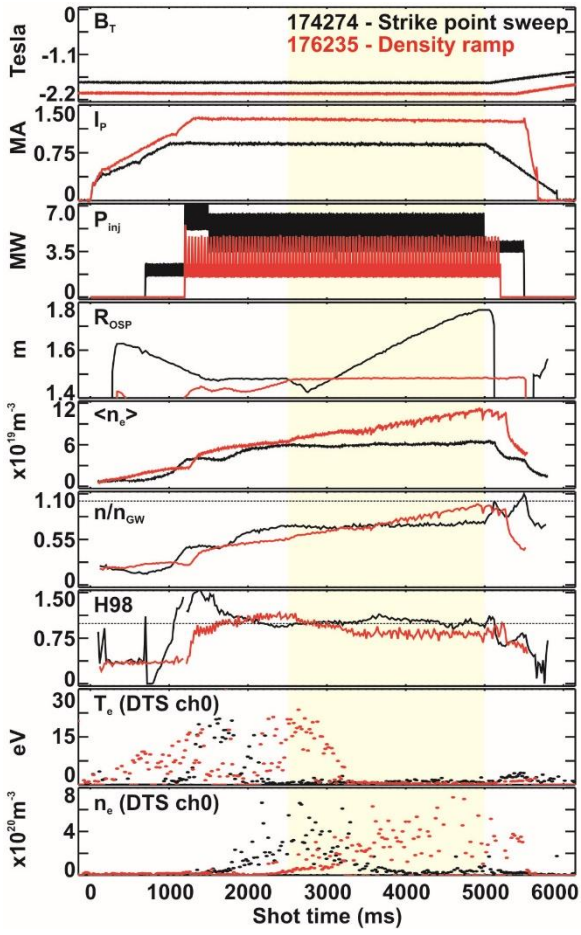

FIG. 2. Representative shot parameters for DivSPRED studies. Yellow region indicates when data is analyzed.

2. CALIBRATION AND SENSITIVITY

To measure the wavelength calibration and instrumental line width for each visible instrument, an HgNe light source was coupled to each spectrometer and line fitting p for the brightest emissions across the visible and NIR spectrums. For the same purpose on the DivSPRED, an electrodeless Krypton VUV source manufactured by Resonance Limited was attached to the instrument. Wavelength calibration of the DivSPRED was also accomplished by identifying both dominant intrinsic emitters including Deuterium and the primary impurity in DIII-D plasmas, Carbon, as well as lines from impurities introduced into the plasma (Ar, Ne, N) that also efficiently radiate at lower wavelengths (20-60 nm). Data were captured at different values of integration times and system gains to confirm stability of each

calibration, and for varying values of MCP and phosphor high voltage on the DivSPRED in order to map the sensitivity versus those values.

For the absolute intensity calibration, a key advantage for using the particular Model 251 available for DivSPRED was that a prior intensity calibration was performed for this spectrometer at the NIST SURF facility [12] where a well-characterized beam of EUV/VUV radiation was used to determine the calibration curve vs. wavelength. While a different camera was employed on the device at the time (an older Reticon-based 1D detector) and the viewing geometry was different, these aspects should only lead to variation in linear scaling of the calibration curve. Thus, the shape of the original calibration may be used in conjunction with calibration using the *in-situ* branching ratio technique, and with knowledge of the changes in gain for the MCP and phosphor.

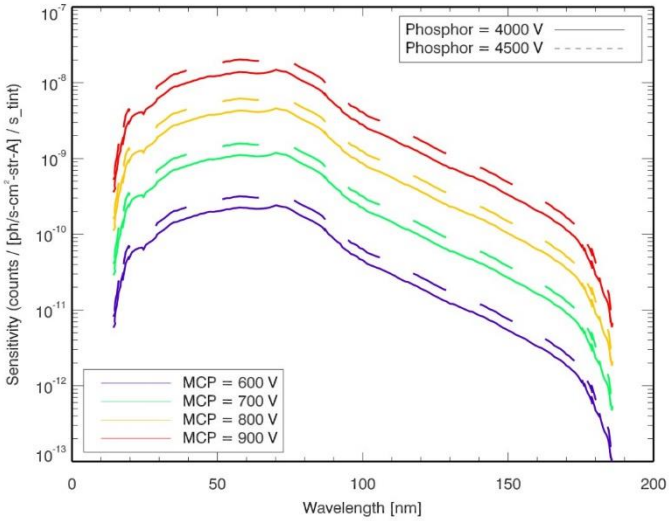

FIG. 3. Spectrometer sensitivity vs. wavelength for DivSPRED with 290 gr/mm grating and increasing MCP and phosphor high voltage.

The branching ratio (BR) technique is a method by which cross calibration between two instruments (or two spectral locations on the same instrument with sufficiently wide bandwidth) may be determined. The technique relies on the simultaneous measurement of two emission lines with the same upper level, wherein the absolute emission intensity of those lines will be proportional only to the ratio of the A_{ki} Einstein emission probability coefficients for the two lines. This ratio will therefore be independent of the plasma parameters in the emitting volume, making it very attractive for use in a complex plasma environment. When one line of the pair is measured with an independently calibrated instrument (where visible calibration is simpler), a proportional calibration may be applied to the second instrument, often for a very different spectral region. For the BR technique applied to DivSPRED, three key transitions with the same upper energy level and with emission lines of significant intensity within the observable bandwidth of the available instruments were employed as listed in Table 2. Benchmarks provided by the BR technique at the EUV/VUV line wavelengths allowed the original NIST SURF calibration curve to be scaled within ±10%. Application of the Ly-β/D_α ratio is of particular interest due to the possibility that opacity of the plasma (i.e., self-absorption of Ly photons) may contaminate the ratio. Analysis of available data at conditions from low to very high line-average density in DIII-D however (up to ~1E20/m^3) show no sign that the ratio changes suggesting that opacity is not a concern up to that density.

TABLE 2. BRANCHING RATIO EMISSIONS FOR DIVSPRED CALIBRATION

Line	**EUV/VUV**			**VIS/NIR**			$\frac{A_{Ki}EUV/VUV}{A_{Ki}VIS/NIR}$
	Transition	λ (nm)	A_{ki} (s^{-1})	Transition	λ (nm)	A_{ki} (s^{-1})	
D I	4→1 Ly-β	102.54429	5.5766E7	4→2 H_α	656.1012	4.4114E7	1.264
C II	$2s^23d\ ^2D \rightarrow 2s^22p\ ^2P^0$	68.7053	2.35E9	$2s^23d\ ^2D \rightarrow 2s^23p\ ^2P^0$	723.132	3.49E7	67.41
		68.7345	2.82E9		723.642	4.18E7	
C III	$2s3d\ ^1D \rightarrow 2s2p\ ^1P^0$	57.4281	6.24E9	$2s3d\ ^1D \rightarrow 2s3d\ ^1D$	569.592	4.27E7	146.1

Unlike the useable range of Silicon-based CCD/CMOS detectors in the visible range (400-700 nm) whose absolute intensity sensitivity typically changes by no more than an order of magnitude, the sensitivity of the SPRED diagnostic is found to vary by three orders of magnitude over the useable spectral range, with sensitivity peaking near 60 nm. While with Si-based detectors the change in sensitivity is due to the variation in quantum efficiency of Si itself, the sensitivity of the SPRED is primarily due to the product of variation in efficiency for the grating and photocathode. In addition, a range of high voltage can be applied to both the phosphor screen (phos) and the multichannel plate (MCP) as explored with DivSPRED to allow for up to over two additional orders of magnitude of sensitivity applied evenly over the extent of the useable bandwidth of the particular grating in use. This change in gain was measured using the Resonance VUV line source after verifying stable emission intensity, altering the MCP and phosphor voltages, and measuring the impact on line intensity as measured by the detector. Results of this study demonstrate a gain increase of 1.5X with each increase of 500V on the phosphor. As well, each increase of 100V on the MCP adds from 3X to 5X the gain. Curves of absolute intensity sensitivity versus wavelength for the DivSPRED are shown in FIG. 3.

3. RESULTS

3.1. Spectra

With the sensitivity calibration applied to raw data, spectra are shown from DivSPRED in FIG. 4 viewing through the outer scrape-off layer (SOL) to the OSP at three points in a plasma discharge with a density ramp. Detachment transition occurs at n/n_{GW}~0.68. Spectra are dominated by a small number of intense emission lines of D I and C II, III, and IV whose rest wavelengths from the NIST atomic database are marked with vertical lines, and labelled in order of Z number from top-down. Less intense emission lines of B, N and O are also identified. Resonance emission lines are labeled in bold with yellow text and dominate each spectra. The spectral radiance of the brightest emission lines including Ly-α and many lines of C increase by nearly an order of magnitude moving from attached conditions ($T_{e,OSP}$~20 eV at n/n_{GW}=0.44) to fully detached conditions ($T_{e,OSP}$=0.4 eV at n/n_{GW}=0.93). The spectra shows no obvious broadband emission such as Blackbody or Bremsstrahlung radiation as is observed in the plasma core by similar EUV instruments at other devices. There are also no indications of metallic impurities as is commonly observed in the SXR/EUV in the core, presumably due to the overwhelming intensity of resonance emissions from the divertor.

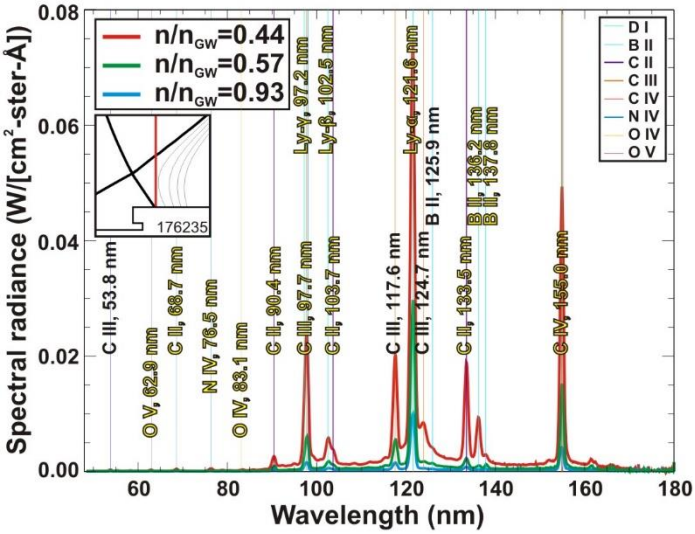

FIG. 4. Spectral radiance with 290 g/mm grating viewing the OSP at various n/n_{GW}. Resonance lines are labeled in bold with yellow text.

3.2. Integrated power vs. bolometry

A useful check on the calibrated EUV/VUV data is to integrate the spectral radiance for the full profile to determine the radiance or the emitted power density in the DivSPRED view and compared that value to separately calibrated data from nearby bolometric chords. Bolometry on DIII-D is composed of a 48-channel platinum-foil array that integrates all radiated power from the plasma, found to be primarily in the VUV and shorter wavelengths [19]. The comparison is shown in a representative plasma discharge with a density ramp, shown in FIG. 5. The DivSPRED data captured at 544 Hz (shown in red) was down-sampled in time to match the 25 Hz rate of the bolometer (yellow). Data from bolometer chords shown in the inset are plotted and, for the majority of the discharge, integrated radiance measured by the DivSPRED falls between those chords, with significant temporal features on each bolometer chord found also on the DivSPRED trace. While the comparison between the two diagnostics is not perfect due to the differing viewing geometry, this approximate agreement in integrated radiance in the EUV/VUV spectrum compared to the full-spectrum radiated power measurement by the foil bolometers is an overall indication that the DivSPRED calibration is accurate.

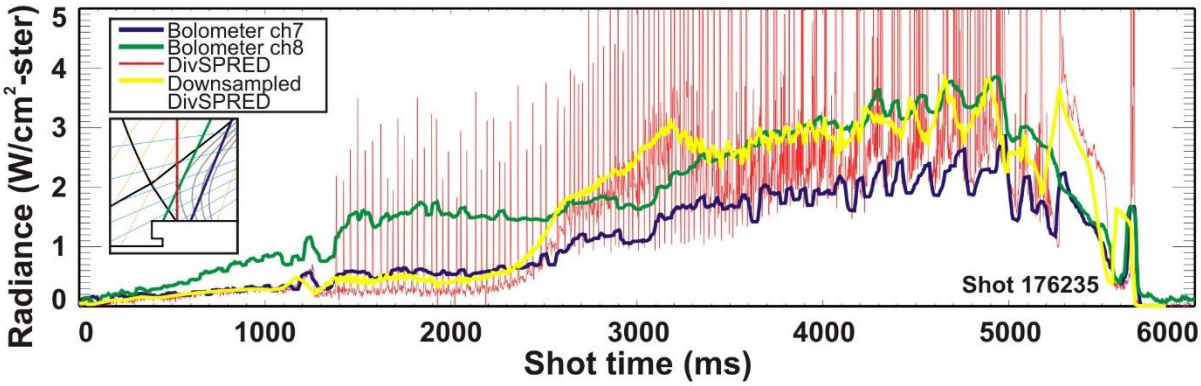

FIG. 5. Integrated radiance through full DivSPRED spectrum for a density ramp discharge. DivSPRED data is taken at 544 Hz (red), then down-sampled to 25 Hz (yellow) to compare to neighboring bolometer channels (green and purple).

4. SPECTRAL ANALYSIS

To quantify the emitted radiance for each species and charge state measured in the DivSPRED spectrum, each emission line is fitted with a Gaussian function for each frame of data (~5000 at the typical 540 Hz capture rate). No attempt is made to use a Lorentzian curve due to observation that the broad width of the instrumental

function for the DivSPRED (0.95 nm FWHM) dominates the shape of the spectra. This fitting is carried out for all of the dominant emissions in the spectra. For ease of visualization, a locally-weighted fit is performed to the data vs. R-R_{sep} and n/n_{GW}, and shown in FIG. 6 without the raw data points. Note that data for C II and C III are each equal to the sum of line radiance from three separate lines. Representative data are shown from discharges shown in FIG. 2 including a broad strike point sweep at constant density (left column) and a density ramp with DivSPRED viewing the OSP (right column). Data are also shown in both absolute line radiance (top row), as well as a fraction of the total line radiance in the spectra. It is apparent that adding each of the 10 most intense lines in the spectra only sums up to ~60% of the spectra-integrated radiance, leaving a significant unaccounted emission source. This observation was not expected based on prior studies of divertor radiation [7]. For the dominant lines, C IV is found to be the most intense throughout most of the divertor in the swept shot. The primary exception is in the SOL outboard of the OSP where D I, Ly-α leads. In the density ramp with the OSP steady at the DivSPRED chord position, Ly-α is also dominant, and remains so throughout the density ramp. This suggests that the species composition after detachment onset does not significantly change as the discharge progresses toward MARFEing conditions. Detachment itself in this field direction (ion B×∇B into the divertor) is characterized by a sudden transition from T_e~8 eV to <2 eV at n/n_{GW}~0.68 (the 'T_e cliff' [20]), at which time there is a coincident change in the trends for the fractional emission from each species monitored by DivSPRED (FIG. 6 lower right).

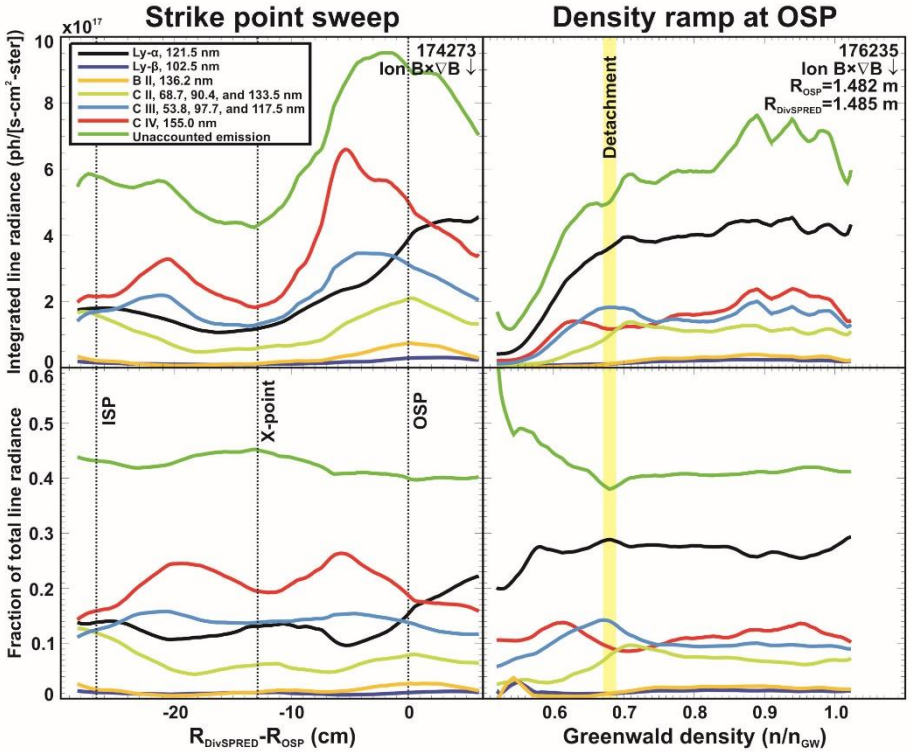

FIG. 6. Integrated line radiance for major emission lines (top) and fractional emission of the total (bottom) for both a strike point sweep at constant density (left) and a density ramp with a steady strike point (right) as measured by DivSPRED.

The portion of the spectra-integrated line radiance not accounted for by the brightest 10 emission lines in the spectra is also shown in each panel of FIG. 6. In order to identify the source of this emission, the same spectral data in FIG. 4 are plotted again in FIG. 7 on a log Y-axis. This reveals a great deal of additional distinguishable emission lines (approximately 40 from a total of 15 species and charge states), and also a broad, persistent emission feature limited to the spectral region of ~90-165 nm region. While the intensity of this feature is low (>10X less than the brightest emission peaks), its broad nature leads to it accounting for a significant portion of the spectra-integrated radiance. One possible explanation for this feature is the band structure for the Lyman B-X and Werner C-X molecular bands of D_2 which also are found at these wavelengths with a very similar

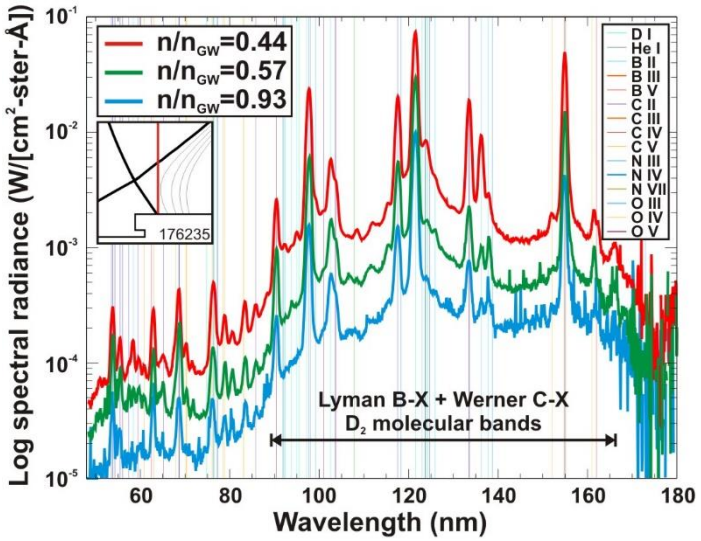

FIG. 7. Same spectral radiance with 290 g/mm grating viewing the OSP at increasing n/n_{GW} as shown in FIG. 3. A log Y-axis reveals many additional emission lines, and a region where Lyman-Werner D_2 bands may account for missing radiation compared to modeling.

intensity structure [21-23]. At the relatively low resolution of the DivSPRED, it is not possible to resolve features in these bands; however, the theoretical spectra convoluted with an ~1 nm instrumental width would result in a block-like emission very similar to that found in FIG. 7. The prospect of such significant portion of the radiated power in the divertor being due to molecular source could help explain why recent integrated divertor modeling with fluid codes has found a shortfall of 50% or more in simulated radiated power compared to bolometric experimental results. These boundary codes – UEDGE, SOLPS, and EDGE-2D – were not run with full inclusion of molecular processes and interactions. It should be noted, however, that another possibility for accounting of some portion of the emission may lie in a very broad but low intensity component of the instrumental function for MCP-based spectrometers which has been observed at other facilities [24]. Uncertainties in the calibration and accounting for the full instrumental function of the instrument are currently being studied.

5. SUMMARY

Absolutely calibrated divertor SPRED on DIII-D provides a critical window into study of dominant resonance emissions that account for >50% of radiated power in the divertor in conditions spanning attached to detached plasmas. Data from this diagnostic, integrated with those from the available spectroscopic suite spanning the EUV, visible and NIR spectrums, as well as divertor Thomson scattering and other imaging and probe-based diagnostics, create a powerful basis for experimental validation of state-of-the-art boundary simulation codes, in particular, the radiation shortfall as discovered with modelling of JET, ASDEX-U and DIII-D. A preliminary conjecture that the unaccounted emission in the 90-165 nm region of the DivSPRED data studied to date is identifiable as Lyman-Werner band emission from D_2 presents an interesting potential resolution of the shortfall, motivating further research in molecular processes in the tokamak boundary including recycling and excitation/breakup rates, and their integration into modelling codes.

ACKNOWLEDGEMENTS

This material is based upon work supported by the U.S. Department of Energy, Office of Science, Office of Fusion Energy Sciences, using the DIII-D National Fusion Facility, a DOE Office of Science user facility, under Awards DE-FC02-04ER54698. DIII-D data shown in this paper can be obtained in digital format by following the links at https://fusion.gat.com/global/D3D_DMP.

REFERENCES

[1] GROTH, M., et al., Nucl. Fusion 53 (2013 093016.
[2] CANIK, J.M., et al., Phys. Of Plasmas 24 (2017) 056116.
[3] FONCK, R.J., RAMSEY, A.T., and YELLE, R.V., Applied Optics 21 12 (1982) 2115-2123.
[4] SOUKHANOVSKII, V.A., KAITA, R., and STRATTON, B., Rev. Sci. Instrum. 87 (2016) 11D605
[5] WOOD, R.D., et al., Proceedings of the 23rd EPS conf. Cont. Fusion and Plasma Phys., June 24-28, 1996, Kiev, Ukraine.
[6] WEST, W.P., et al., Plasma Phys. Control. Fusion 39 (1997) A295-A310.
[7] ISLER, R.C., et al., Physics of Plasmas 4 (1997) 355-368.
[8] FENSTERMACHER, M.E., Phys of Plasmas 4 (1997) 1761-1770.
[9] WEST, W.P. et al., J. Nucl. Mater. 266-269 (1999) 732-738.
[10] PORTER, G.D., et al., Phys. Of Plasmas 7 (2000) 3663.
[11] MUMMA, M.J. and ZIPF, E.C., J. of the Optical Society of America 61 1 (1971) 83-88.
[12] WOOD, R.D., and ALLEN, S.L., Rev. Sci. Instrum. 59 8 (1988) 1537-1543.
[13] GREICHE, A., et al., Rev. Sci. Instrum. 79 (2008) 093504
[14] LAWSON, K.D., et al., J. Instrum. 4 (2009) P04013.
[15] DONG, C., et al., Rev. Sci. Instrum. 81 (2010) 033107.
[16] MUNOZ BURGOS, J.M., et al., Phys. Of Plasmas 22 (2015) 123301.
[17] ZHANG, L., et al., Rev. Sci. Instrum. 86 (2015) 123509.
[18] GUIRLET, R., et al., Journal of Instrum. 12 (2017) P01006.
[19] LEONARD, A.W., et al., Rev. Sci. Instrum. 66 2 (1995) 1201-1204.
[20] McLEAN, A.G., et al., J. Nucl. Mater. 463 (2015) 533.
[21] SAWADA, K., and GOTO, M., Atoms 4 29 (2017) 1-26.
[22] FANTZ, U., et al., Plasma Sources Sci. Technol. 25 (2016) 045006.
[23] HOLLMANN, E.M., et al., Plasma Phys. And Control. Fusion 48 (2006) 1165.
[24] LAWSON, K.D., EURATOM/CCFE Fusion Association, personal communication, 2018.